Nuclear Instruments and Methods in Physics Research A 812 (2016) 12–16

Contents lists available at ScienceDirect

Nuclear Instruments and Methods in Physics Research A

journal homepage: www.elsevier.com/locate/nima

Electrodeposition of uranium and thorium onto small platinum electrodes

Michael A. Reichenberger [a,*], Takashi Ito [b], Philip B. Ugorowski [a], Benjamin W. Montag [a], Sarah R. Stevenson [a], Daniel M. Nichols [a], Douglas S. McGregor [a]

[a] S.M.A.R.T. Laboratory, Mechanical and Nuclear Engineering Dept., Kansas State University, Manhattan, KS 66506, USA
[b] Department of Chemistry, Kansas State University, 213 CBC Building, Manhattan, KS 66506-0401, USA

ARTICLE INFO

Article history:
Received 18 August 2015
Accepted 21 December 2015
Available online 31 December 2015

Keywords:
Neutron detector
Reactor instrumentation
Electrodeposition
Fission chamber
Micro-Pocket Fission Detector
MPFD

ABSTRACT

Preparation of thin U- and Th-coated 0.3 mm diameter Pt working electrodes by the cyclic potential sweep method is described. Uranyl- and thorium hydroxide layers were electrodeposited from ethanol solutions containing 0.02 M natural uranyl and 0.02 M natural thorium nitrate, each with 3.6 M ammonium nitrate. The cell for electrodeposition was specially developed in order to accommodate the small working electrodes for this research by including a working electrode probe, 3-D translation stage, and microscope. The source material deposition was analyzed using digital microscopy and scanning electron microscopy, and confirmed using x-ray fluorescence measurements. The appropriate potential range for electrodeposition was determined to be −0.62 V to −0.64 V for a 0.3 mm diameter Pt working electrode placed 1 cm from the counter electrode. Smooth, uniform deposition was observed near the central region of the working electrode, while surface cracking and crystalline formations were found near the edge of the working electrode. The final procedure for sample substrate preparation, electrolytic solution preparation and electrodeposition are described.

1. Research motivation

The accurate deposition of thin U and Th layers onto small metal electrodes is essential for the continued development of Micro-Pocket Fission Detectors (MPFDs) [1]. MPFDs are under development, which are constructed of materials resistant to the high-neutron flux and high-temperature environment present in the core of many research nuclear reactors. Specifically, MPFDs do not significantly perturb the local neutron flux, while providing a real-time measurement of critical reactor parameters, and are capable of continuous operation during extended testing periods. The small size, low sensitivity, and desired lifetime of MPFDs necessitates a reliable method of electrodeposition of very thin layers of neutron-sensitive materials onto radiation-hard substrate materials [1,2]. Typical MPFDs require deposition thicknesses of 350 $\mu g\,cm^{-2}$ onto substrates $< 1.0\,mm^2$. The effectiveness of electrodeposition of U and Th onto 0.3 mm diameter evaporated platinum electrodes on silicon substrates was analyzed. Although MPFDs are typically constructed with alumina substrates, silicon substrates were examined in this study for their ease in manufacturing and smooth surface finish. The plating cell was developed in order to facilitate samples of substrate and electrode dimensions as described. Natural U and Th are desired for current MPFD fabrication [2]. Uranium and thorium salts were used as source material for the electrolytic solutions.

Typical methods of surface deposition of U and Th compounds include vacuum evaporation, electro-spraying, painting with an organic solution, electrodeposition, and direct drop precipitation [3]. Electrodeposition methods are commonly used to prepare actinide layers onto targets for use as alpha particle sources and ion beam targets [3–5]. The use of nitrate-rich solutions with organic solvents (isopropyl alcohol [4] and acetone [3]) has been reported for electrodeposition preparation of target materials. Electrodeposition from organic solutions offered a very uniform layer, but often suffered from poor reproducibility [5]. Electrodeposition methods are commonly optimized from the viewpoint of the maximum efficiency of the electrodeposition, but depend heavily on electrochemical cell design [4,5]. Still other methods have been developed for rapid preparation of source material for nuclear waste analysis [3]. Both of the previous methods call for working electrodes on the order of several square centimeters. However, the objective of the present work is to deposit precise amounts of U and Th on very small electrodes ($< 1\,mm^2$) for use as MPFD substrates. Although much of the chemistry from previous methods can be used to aid in the development of MPFD substrates, the electrodeposition method is being applied with a

* Corresponding author.
E-mail address: mar89@ksu.edu (M.A. Reichenberger).

http://dx.doi.org/10.1016/j.nima.2015.12.046
0168-9002/

different objective. In contrast to many other methods which strive for high electrodeposition efficiency, high precision and reproducibility is important for the development and testing of MPFDs. The neutron-reactive coating for MPFDs must be precisely deposited in order properly balance U and Th content to maximize device lifetime [6].

Here, uranyl and thorium hydroxide layers were electrodeposited onto small Pt disk electrodes using the cyclic potential sweep method [7]. The hydroxide layers were deposited by taking advantage of an increase in pH at the vicinity of the electrodes as a result of the reduction of nitrate [8]. The cyclic potential sweep method provides a more controlled means for such electrochemically assisted deposition as compared to the more commonly used potential-step method for the following two reasons. First, this method facilitates applying a potential required for nitrate reduction for the shorter period of time by adjusting potential sweep rate. The longer application of the cathodic potential using the potential-step method generates large gas bubbles on the electrodes due to side reactions such as the reduction of water, preventing the deposition of uniform hydroxide layers. The cyclic potential sweep permits the repetitive application of the cathodic potential for the shorter period of time to induce a sufficient pH increase with minimum formation of large gas bubbles. Second, the deposition of the hydroxide layers can be monitored from the cathodic current recorded during the repetitive potential sweep. The deposition of insulating hydroxide layers leads to a decrease in the cathodic current due to the reduced exposure of the active Pt electrode area. After determining the appropriate potential sweep range, the number of potential segments can be adjusted to deposit a precise amount of U or Th material onto the Pt electrode. The present work developed an electrochemical cell appropriate for work with very small working electrodes and determined the effectiveness of the cyclic potential sweep method for the fabrication of MPFD substrate materials.

2. Experimental method

The production of sample MPFD substrates with thin U and Th coatings consisted of three primary steps: electrode fabrication, solution preparation, and electrodeposition.

2.1. Electrode fabrication

Electron beam evaporation was used to deposit metal contacts onto insulating substrates for electrodeposition testing. Shadow masks were used to create samples with circular electrodes as depicted in Fig. 1. Custom nickel shadow masks were manufactured at the Kansas State University Multiphase Microfluidics Laboratory using a Minitech Mini-Mill 3 micro-milling machine. The present work used 0.3 mm diameter, circular electrodes evaporated onto silicon dioxide substrates. Silicon dioxide was chosen for its smooth surface and ease in processing post-evaporation.

Prior to evaporation, each 3-in. silicon wafer was cleaned using a 5-min bath in each of acetone and isopropyl alcohol, followed by a 1-min buffered oxide etch and 5-min de-ionized water bath. The wafer was then dried using pressurized nitrogen gas. The custom shadow mask was fixed to the surface of silicon wafer just before insertion into the evaporation chamber. A 50 Å Ti evaporation was used to aid in the adhesion of the Pt layer. Afterwards, a 500 Å Pt layer was evaporated as the primary electrode material. Platinum was used due to its high melting point, resistance to corrosion, and low neutron-absorption cross-section [9]. Samples which did not utilize a thin Ti adhesion layer suffered from complete electrode material loss during the wafer dicing process. Wafer processing and evaporation was conducted in the class-100 cleanroom facility

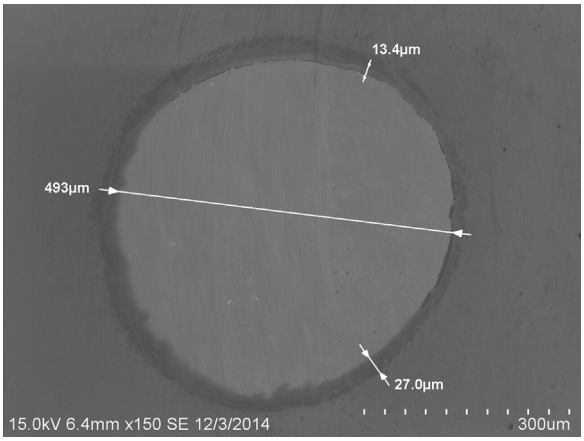

Fig. 1. SEM image of a circular Pt electrode prior to electrodeposition. The size and shape of each sample was verified after evaporation.

Table 1
Compositions of solutions used for electrodeposition of uranyl and thorium hydroxide layer on Pt electrodes.

Component	0.02 M $UO_2(NO_3)_2$	0.02 M $Th(NO_3)_4$
Uranyl or thorium nitrate	410 mg	480 mg
Ammonium nitrate	14,410 mg	14,410 mg
190 Proof ethanol	5.78 mL	5.78 mL
Measured solution pH	3.4	3

at the Kansas State University S.M.A.R.T. Laboratory. Following electrode evaporation, the wafers were diced into 5 mm × 5 mm square samples for electrodeposition testing. The samples were visually inspected for surface quality using a Hitachi S-3400N scanning electron microscope, as depicted in Fig. 1.

2.2. Solution preparation

Uranyl nitrate hexahydrate (99.9%) and thorium nitrate hydrate (99.8%) were used as the respective sources of U and Th for each electrodeposition. The composition of the solutions used for U and Th deposition differed only in the quantities of uranyl nitrate and thorium nitrate. Prior to solution preparation, all of the glassware was cleaned using HNO_3, acetone, isopropyl alcohol, and a de-ionized water bath. The U/Th nitrate and ammonium nitrate were weighed using an Ohaus AR0640 scale, combined into a 250 mL beaker, and de-ionized water was added to bring the solution to 100 mL. A 25 mL ethanol/de-ionized water solution was then prepared and added to the U/Th nitrate and ammonium nitrate solution. The solution was placed on a magnetic stirring plate on a low (3 of 10) stirring setting. The final solution was then topped off to 150 mL with de-ionized water and a pH measurement was taken using a calibrated Thermo Scientific Orion 3-Star pH monitor. The amount of each material used for the solution preparation and measured pH are shown in Table 1. The U solution possessed a slight yellow tint, while the Th solution was clear as depicted in Fig. 2. Precipitation of the U solution was observed after several days. Thus, fresh electrolytic solution was prepared for each electrodeposition batch, and the electrodeposition was conducted immediately after solution preparation.

2.3. Electrodeposition via the cyclic potential sweep method

Samples were rinsed with isopropyl alcohol prior to electrodeposition. The CH Instruments CHI600E potentiostat used for the present work utilized an electrochemical cell with three

Fig. 2. Prepared solutions of 0.02 M $UO_2(NO_3)_2$ (left) and 0.02 M $Th(NO_3)_4$ (right).

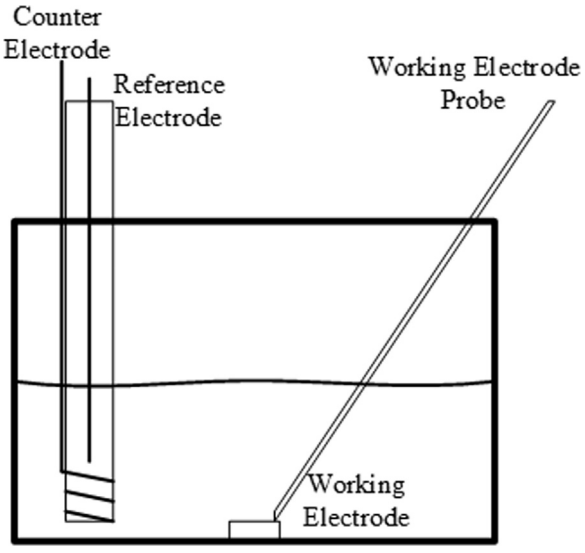

Fig. 3. Schematic illustration of the electrochemical cell consisting of a reference electrode, count electrode, and working electrode.

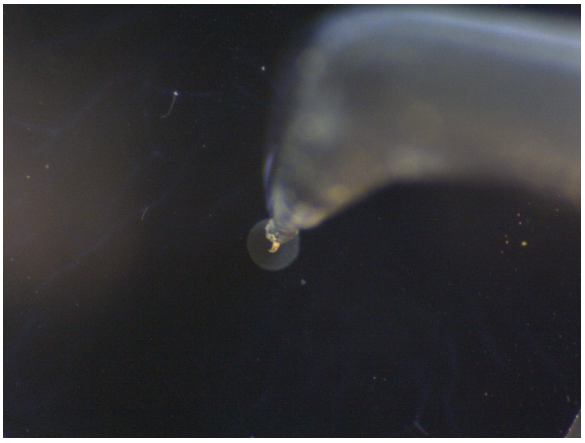

Fig. 4. An optical microscope image of a Pt electrode with the working electrode probe prior to electrodeposition. Proper alignment of the working electrode probe and Pt electrode was necessary before electrodeposition was possible.

electrodes. The electrochemical cell which was developed to accommodate the small electrode design included a 3-dimensional translation stage, counter/reference electrode assembly, working electrode probe, and Leica DMS300 microscope. The counter/reference electrode assembly was constructed using an Ag/AgCl reference electrode submerged in 3.0 M KCl inside a glass vial. The counter electrode (0.013 in. diameter 99.95% Pt wire) was then wrapped around the reference electrode glass vial as shown in Fig. 3. The 5 mm × 5 mm silicon sample with evaporated Pt working electrode and the counter electrode/reference electrode assembly were placed into a glass petri dish. Electrolytic solution was added to submerge both the silicon sample and the counter electrode. The stainless steel working electrode probe was insulated with exception of the tip to enable electrical contact with the working electrode, visible in Fig. 4. The 3-D stage was then adjusted to establish contact between the Pt electrode on the silicon sample and the working electrode probe, also depicted in Fig. 4. After electrical contact was established, U/Th was deposited onto the working electrode surface.

Determination of the optimal parameters required numerous trials, however a potential sweep from −0.62 V to −0.64 V was determined to yield the most consistent surface deposition using a 0.01 Vs^{-1} sweep rate. Voltages beyond −0.64 V produced severe bubble generation and yielded more unwanted crystalline deposits on the surface of the working electrode. Additionally, no electrodeposition was observed from 0 V to −0.62 V. The present work tested the effectiveness of electrodeposition with 500 potential sweep segments. The electrodeposition was performed at room temperature (typically below 28 °C). The cyclic potential sweep process yielded current-voltage plots (cyclic voltammograms) representative of those depicted in Fig. 5 for uranyl-nitrate and thorium-nitrate solutions. All samples were rinsed with isopropyl alcohol after electrodeposition and allowed to dry before storage in individual sealed plastic bags.

3. Results and surface analysis

During each potential sweep segment, a small amount of insulating U/Th hydroxide was deposited onto the working electrode surface. As additional material was deposited, the electrochemically active surface area of the working electrode decreased

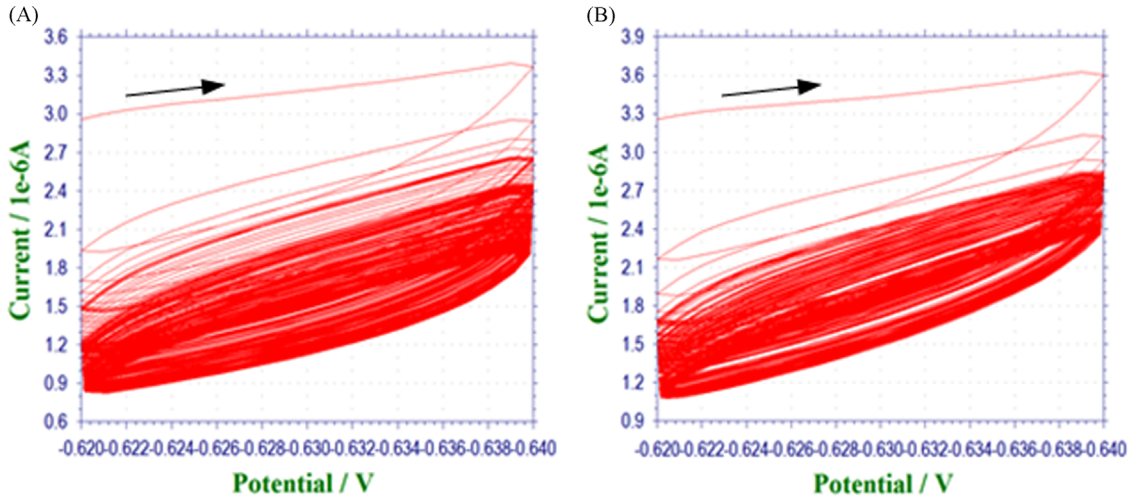

Fig. 5. Current vs potential plots measured at the sweep rate of 0.01 vs −1 in (A) 0.02 M $UO_2(NO_3)_2$ and (B) 0.02 M $Th(NO_3)_4$. The cathodic current gradually decreased as a result of the repetitive potential sweep due to the deposition of a (A) $UO_2(OH)_2$ (A) and (B) $Th(OH)_4$ layer on the Pt electrode surface.

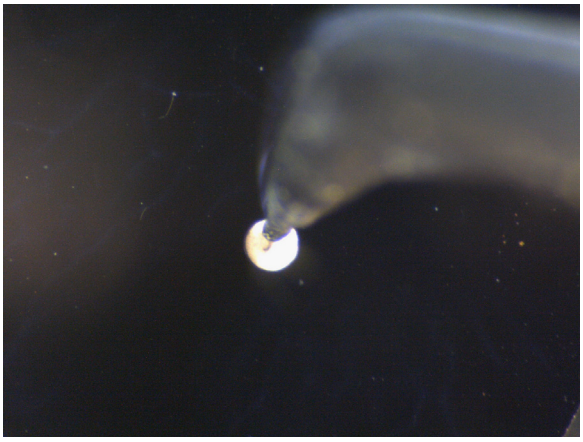

Fig. 6. Optical microscopy image of a Pt electrode after electrodeposition of the Th hydroxide. The electrode surface slowly changed color during the electrodeposition from silver (Pt) to white (Th).

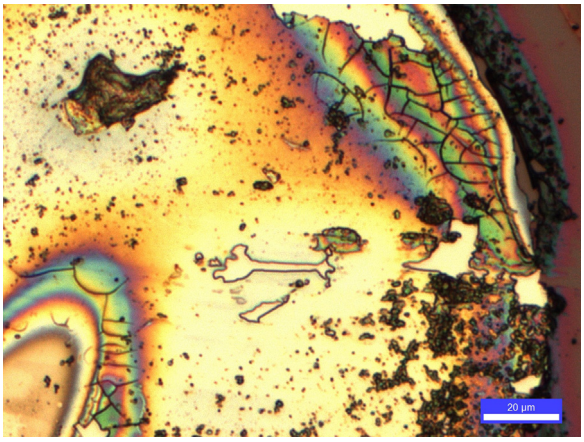

Fig. 7. Optical microscopy image of a Pt electrode after U electrodeposition. Surface cracking and crystalline formation is visible near the perimeter of the electrode.

to give a smaller cathodic current, as shown in Fig. 5. Small bubbles occasionally formed at the contact point of the working electrode probe and working electrode surface but quickly detached. The deposited material was clearly visible as the Pt surface changed in color from silver to yellow (U) and white (Th). A plated Th sample just after electrodeposition is shown in Fig. 6. Digital microscopy, scanning electron microscopy (SEM), and x-ray fluorescence (XRF) analysis were all used to determine the effectiveness of the electrodeposition process.

A Leica DVM 2500 microscope was used to visually inspect each sample. The color of the samples indicated areas where U- or Th-hydroxides were deposited. Uranium samples had golden-colored electrode surfaces while Th samples had white-colored electrode surfaces. Special notes were taken of any regions where the electrode surface appeared absent of deposited material. Some samples exhibited crystalline depositions around the perimeter of the electrode surface as shown in Fig. 7.

The SEM was used to examine the surface features of the samples after electrodeposition, showing three distinct regions depicted in Fig. 8. The first region was a smooth, conformally coated region located in the center of the sample and extending radially as depicted in Fig. 8(A). Near the edges of the samples, a cracked layer was observed, shown in Fig. 8(B). The crystalline formations depicted in Fig. 7 were also observed in the same region as the surface cracking. The crystalline depositions were

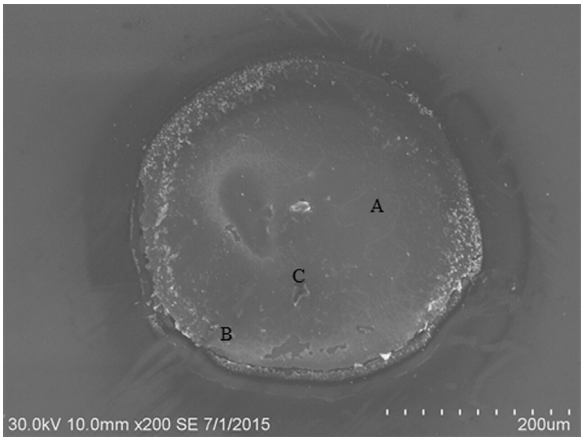

Fig. 8. SEM image of a U-deposited Pt electrode showing three distinct regions: (A) a uniformly deposited region, (B) a region with thick deposition layers, and (C) an undeposited region.

observed to detach easily by coming in contact with the plastic container in which the samples were stored. The cracked region was preferentially observed on the side closest to the counter electrode. XRF analysis of the cracked region suggested larger amount of U/Th in the cracked region. Finally, regions were observed on each sample where little or no deposition had taken

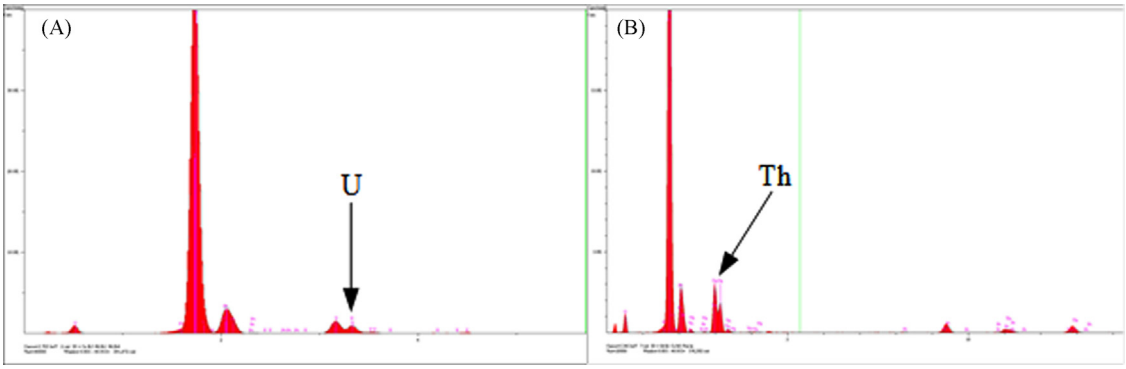

Fig. 9. XRF spectrum measured at the surface of a (A) U- and (B) Th-deposited Pt electrode. Numerous U characteristic x-ray peaks were clearly present. Peaks for Pt, Si, and O are also present due to the penetration of x-rays from the substrate through the thin electrodeposited layer.

Table 2
XRF results representing the relative abundance of four elements on U-deposited and Th- deposited Pt electrodes ($\sim$ 150 μm × 150 μm for each region).

Sample and region	Si concentration (wt%)	Pt concentration (wt%)	O concentration (wt%)	U / Th concentration (wt%)
U Central Region	64	6	21	9
U Cracked Region	61	11	15	13
Th Central Region	78	10	11	1
Th Cracked Region	53	9	16	22

place shown in Fig. 8(C). These regions varied in size and shape but are possibly due to surface contamination (dust particles for example), probe contact, or detachment of a hydroxide layer.

X-ray fluorescence measurements were used as a qualitative assessment of the amount of U or Th deposited on each sample. Measurements were conducted for each of the regions of interest for each sample. The relative abundance of each sample material was calculated based on the XRF measurement results. Silicon, oxygen, and platinum were also included in the surface composition estimate due to the penetrating ability of the SEM electron beam and subsequent characteristic x-rays. Clear peaks were present in the XRF spectra depicted in Fig. 9 for U and Th. Results of XRF analysis for each region for a characteristic sample are summarized in Table 2. The XRF results clearly indicate deposition of both U and Th onto the electrode surface, but also suggest that thicker deposition occurs near the perimeter of the working electrode.

4. Conclusions

Uranium and thorium hydroxides were successfully deposited on 0.3 mm diameter circular Pt electrodes on a silicon dioxide substrate using the cyclic potential sweep method. Digital microscopy, SEM, and XRF have all been used to analyze the surface of the Pt electrodes after electrodeposition. The exact composition of the surface deposition is unknown at this time, but is likely to be uranyl and thorium hydroxide considering the mechanism of the electrodeposition. Crystalline formations of higher U and Th content were found near the perimeter of the electrode surfaces, likely due to the higher electric field strength and enhanced diffusion of ions near the edge of the metal electrode. This effect was observed to be even more prominent on the side of the electrode which was closest to the counter electrode. The effectiveness of electrodeposition will depend heavily upon the electrode size and shape. The central region of the Pt electrodes exhibited a conformal coating of U/Th compounds as verified by XRF analysis. Mass measurements of U and Th coated samples are currently under investigation. The number of sweep segments will also likely affect the amount of U/Th which is deposited on the working electrode and is currently being characterized.

Acknowledgments

Portions of this work have been supported by the US Department of Energy Office of Nuclear Energy under DOE-NE Idaho Operations Office Contract DE-AC07 05ID14517 & US Department of Energy Office of Nuclear Energy under DE-NE0008305. The authors would like to thank Dr. Amy Betz and the Kansas State University Multiphase Microfluidics Laboratory for use of equipment and assistance in machining shadow masks for this work.

References

[1] T. Unruh, J. Daw, K. Davis, D. Knudson, J. Rempe, M. Reichenberger, P. Ugorowski, D. McGregor, J.F. Villard, Charlotte, Enhanced micro pocket fission detector evaluations, in: NPIC & HMIT, Charlotte, NC, 2015.
[2] T. Unruh, J. Rempe, D.S. McGregor, P.B. Ugorowski, M.A. Reichenberger, NEET Micro-Pocket Fission Detector-FY 2013 Status Report, Idaho National Laboratory (INL), Idaho Falls, 2013.
[3] L.C. Hao, C.V. Tao, N.V. Dong, H.N. Nghi, P.T. Dung, L.V. Thong, Kerntechnik 75 (6) (2010) 381.
[4] R.A. Henderson, J.M. Gostic, J.T. Burke, S.E. Fisher, C.Y. Wu, Nuclear Instruments and Methods in Physics Research Section A 655 (2011) 66.
[5] C. Ingelbrect, A. Moens, R. Eykens, A. Dean, Nuclear Instruments and Methods in Physics Research Section A 397 (1997) 34.
[6] M.A. Reichenberger, P.B. Ugorowski, J.A. Roberts, D.S. McGregor, First-order numerical optimization of fission-chamber coatings using natural uranium and thorium, in: Proceedings of IEEE Nuclear Science Symposium, Seattle, WA, 2014.
[7] K. Hosokawa, M. Matsunaga, Y. Tsuru, N. Uemura, Denki Kagaku 53 (2) (1985) 153.
[8] N.I. Kovtyukhova, T.E. Mallouk, Chem. Mater. 22 (2010) 4939.
[9] National Nuclear Data Center, Evaluated Nuclear Data File (ENDF), Brookhaven National Laboratory, 2014.